Chemical Science

ROYAL SOCIETY OF CHEMISTRY

EDGE ARTICLE

View Article Online
View Journal | View Issue

Check for updates

Cite this: *Chem. Sci.*, 2020, **11**, 1335

All publication charges for this article have been paid for by the Royal Society of Chemistry

Received 21st November 2019
Accepted 13th December 2019

DOI: 10.1039/c9sc05908c

rsc.li/chemical-science

Hydrophosphination of boron–boron multiple bonds†

Tom E. Stennett,[ab] Arumugam Jayaraman,[ab] Tobias Brückner,[ab] Lea Schneider[ab] and Holger Braunschweig *[ab]

Five compounds containing boron–boron multiple bonds are shown to undergo hydrophosphination reactions with diphenylphosphine in the absence of a catalyst. With diborenes, the products obtained are highly dependent on the substitution pattern at the boron atoms, with both 1,1- and 1,2-hydrophosphinations observed. With a symmetrical diboryne, 1,2-hydrophosphination yields a hydro(phosphino)diborene. The different mechanistic pathways for the hydrophosphination of diborenes are rationalised with the aid of density functional theory calculations.

Introduction

Compounds containing covalent bonds between phosphorus and boron, while not enjoying the ubiquity of their nitrogen–boron analogues, display a rich chemistry.[1–3] Phosphinoboranes – that is, compounds of the form $R_2B{=}PR'_2$ [4] with a planar geometry at phosphorus and partial double bond character[5] – can undergo addition reactions with such substrates as H_2,[6,7] ketones[6] and dienes[6] and coordinate in an η^2 fashion to transition metals.[8] Borylphosphines, in which the boron atom is not π-acidic (*e.g.* due to π-donor or carborane substituents) and phosphorus thus retains its lone pair and tetrahedral geometry, are highly electron rich η^1 ligands for transition metal complexes.[9–11] By far the most common route for the construction of P–B bonds is salt elimination[12–19] using an alkali metal phosphide, MPR_2, and a haloborane (Scheme 1A), although other routes are known, including nucleophilic addition of a boryl anion to a chlorophosphine (B),[20] elimination of silyl halide (C),[10,11,21] and cross-coupling of a B–I species with secondary phosphines using a palladium catalyst (D).[9]

Of the different synthetic options for the construction of phosphorus–carbon bonds, hydrophosphination of unsaturated carbon substrates has gained popularity in recent years.[22–24] Advantages of this method over typical nucleophilic addition reactions include reduced waste (hydrophosphination is a 100% atom-economical process) and increased functional group tolerance due to the avoidance of highly reactive Grignard or organolithium reagents. However, these reactions typically require a catalyst in the form of a base or metal complex, or a radical initiator, and the scope is somewhat limited in terms of which secondary phosphines can be used. Whereas P–H bond activation at transition[25] and main-group[26] metal centres is well documented, to the best of our knowledge the sole reported example of hydrophosphination of a homonuclear double bond comprising elements other than carbon is the 2016 report by Wang and Wu of hydrophosphination of the

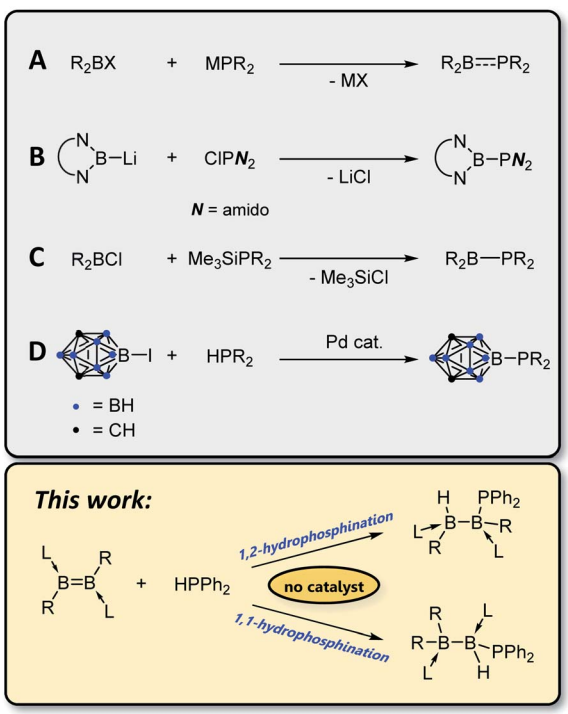

Scheme 1 Reported methods for the construction of covalent boron–phosphorus bonds.

[a]Institut für Anorganische Chemie, Julius-Maximilians-Universität Würzburg, Am Hubland, 97074 Würzburg, Germany. E-mail: h.braunschweig@uni-wuerzburg.de
[b]Institute for Sustainable Chemistry & Catalysis with Boron, Julius-Maximilians-Universität Würzburg, Am Hubland, 97074 Würzburg, Germany

† Electronic supplementary information (ESI) available. CCDC 1954176–1954180. For ESI and crystallographic data in CIF or other electronic format see DOI: 10.1039/c9sc05908c

N=N bond in azobenzene with diphenylphosphine oxide.[27] Recent studies in our laboratories have demonstrated the feasibility of adding H–H,[28,29] B–H,[30–32] B–B,[33,34] S–S[35,36] and Se–Se[35] bonds across boron–boron multiple bonds. In this work, we show that uncatalysed hydrophosphination of both diborenes and diborynes can be used as a mild, selective and catalyst-free route to construct B–P bonds.

Results and discussion

Diborenes based on a chelating benzylphosphine group[37] that holds the aryl substituent in the plane of the boron–boron π-bond have shown particularly high reactivity towards dienes[38] and diboranes,[33] so we chose these compounds as a starting point. The symmetrical diborene **1** was treated with diphenylphosphine at room temperature, leading to slow conversion to a compound with signals in the ^{11}B NMR spectrum at −15.9 and −27.2 ppm, both in the region expected for four-coordinate boron atoms. Heating the mixture to 60 °C for 1 h resulted in the decolouration of the solution and full conversion to the product, which was isolated as a colourless solid after workup in 79% yield. X-ray diffraction on single crystals grown from a diethyl ether solution confirmed the structure as that of product **5**, the result of a 1,2-hydrophosphination across the B=B bond (Scheme 2 and Fig. 1). The PPh_2 and hydrogen substituents display a gauche conformation, while the benzylphosphine units have reverted to a vicinal (1,2-) coordination mode; in contrast to other compounds bearing this substituent,[38] no conversion to the geminal isomer was observed. At 2.051(2) Å, the B1–P1 bond is in the range of published base-stabilised borylphosphines,[15] and markedly longer than both dative B–P bonds in the molecule (B1–P2 = 2.008(2), B2–P3 = 1.928(2) Å). As expected, P1 is highly pyramidal, with a sum of angles of 312.4°. In the ^{1}H NMR spectrum,

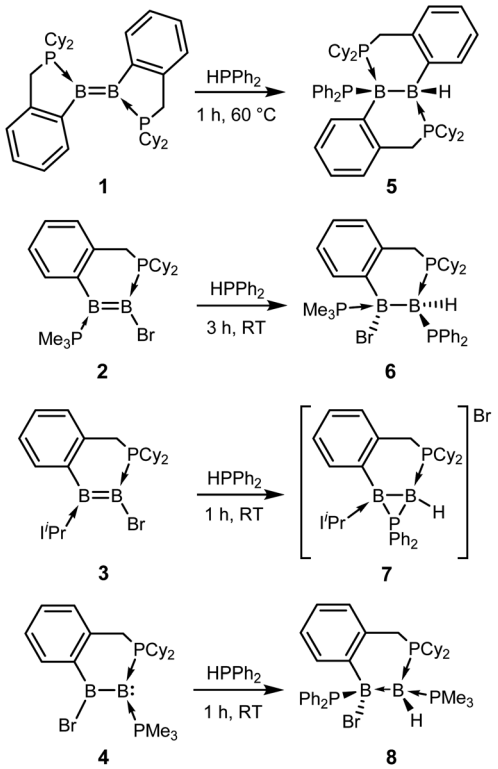

Scheme 2 Hydrophosphination of diborenes and a borylborylene with diphenylphosphine. I^{i}Pr = 1,3-diisopropylimidazol-2-ylidene.

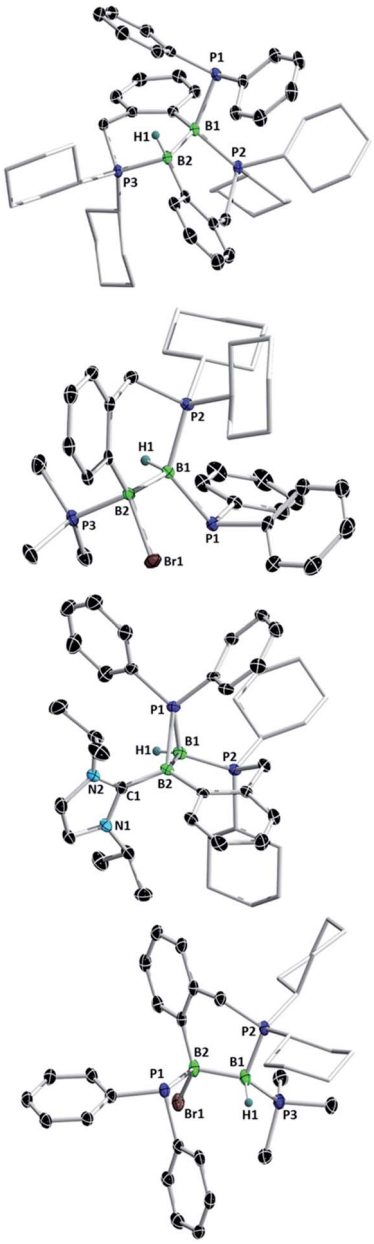

Fig. 1 Molecular structures of (top to bottom) **5**, **6**, **7** and **8**, with selected atomic displacement ellipsoids at the 50% probability level. Hydrogen atoms except for those bound to boron, a bromide counterion (compound **7**) and co-crystallised solvent molecules are omitted for clarity. Selected bond lengths (Å), angles and torsions (°): compound **5**: B1–B2 1.780(2), B1–P1 2.051(2), B1–P2 2.008(2), B2–P3 1.928 (2), P1–B1–B2–H1 24.7(9); compound **6**: B1–B2 1.777(3), B1–P1 1.974(2), B1–P2 1.932(2), B2–P3 1.953(2); compound **7**: B1–B2 1.772(5), B1–P1 1.918(4), B2–P1 1.948(4), B1–P2 1.885(4), B2–C1 1.601(5), B1–P1–B2 54.6(2) P2–B1–B2–C1 141.1(3); compound **8**: B1–B2 1.789(4), B2–P1 1.986(4), B1–P2 1.938(3), B1–P3 1.935(4).

a multiplet centred at 3.08 ppm becomes visible upon ^{11}B decoupling, corresponding to the newly formed B–H group. Two signals at 10.4 ppm and 6.1 ppm in the ^{31}P NMR spectrum correspond to the now inequivalent benzylphosphine phosphorus atoms, whereas the PPh_2 group is represented by a broad signal at −13.3 ppm.

Unsymmetrically-substituted diboron compounds are known to display higher reactivity than their symmetrical counterparts.[39,40] We have previously shown that unsymmetrical diborenes **2** and **3** (Scheme 2) react more quickly than **1** in diboration reactions with B_2cat_2.[33] Treatment of compound **2** with $HPPh_2$ resulted in complete conversion to a new compound within 3 h at room temperature. Signals in the ^{11}B NMR spectrum at −7.7 and −34.2 ppm again indicated the presence of inequivalent, four-coordinate boron atoms. Three broad signals in the ^{31}P NMR spectrum at 23.1, 13.8 and −6.9 ppm also suggested three boron-bound phosphorus environments. Measurement of a ^{1}H NMR spectrum with selective ^{11}B decoupling (δ_{11B} offset = 34 ppm) again revealed a complex multiplet for a B–H moiety at 2.15 ppm. X-ray diffraction confirmed the product as **6**, the result of a formal 1,1-hydrophosphination rather than the expected 1,2-addition across the double bond (Fig. 1). The B1–B2 distance (1.777(3) Å) and B–P distances (B1–P1 = 1.974(2), B1–P2 = 1.932(2), B2–P3 = 1.953(2) Å) lie in the respective expected ranges. N-Heterocyclic-carbene (NHC) supported diborene **3** also undergoes a rapid reaction with $HPPh_2$ at room temperature to give a compound with ^{11}B NMR signals at −21.6 and −37.6 ppm. In this case however, a sharp doublet in the ^{31}P NMR spectrum at −70.9 ppm alongside a broader signal at 8.9 ppm suggested a different outcome. The insolubility of the compound in benzene and tetrahydrofuran also led us to suspect an ion-separated structure. Single crystals obtained from a dichloromethane/pentane solution allowed determination of the structure by X-ray diffraction (Fig. 1), which confirmed the compound to be cationic diborane(5) **7**, bearing a Br^- counterion. Here, the PPh_2 unit bridges the two boron atoms almost symmetrically (B1–P1 = 1.948(4) Å, B2–P1 = 1.918(4) Å). Such three-membered rings are far from common – the only structurally characterised examples of non-cluster B_2P rings are the butterfly-shaped B_2P_2 diradicals reported by Bertrand and co-workers.[41–43]

As reported recently, compound **2** rearranges upon heating to its more thermodynamically stable isomer, **4**, which possesses a polarised boron–boron bond and a borylborylene resonance form.[37] Whereas one might expect such a compound to undergo 1,1-addition reactions to the "borylene" boron atom, both **4** (ref. 33) and a related compound reported by Kinjo's group[44] give 1,2-addition products with B_2cat_2. Compound **4** reacts instantaneously with $HPPh_2$ upon solvation in C_6D_6 to give different NMR signals to those seen in the corresponding reaction with **2**. In the ^{11}B NMR spectrum, two signals at 1.5 and −33.4 ppm are observed, whereas the ^{31}P NMR spectrum reveals two broad signals at 16.4 and −7.8 ppm and a pseudo-triplet at −20.5 ppm. Reduction of the volume of the reaction mixture gave single crystals of the product, which were shown by X-ray diffraction to be 1,2-hydrophosphination product **8** (Fig. 1). As with the diboration product of **4**, compound **8** can be drawn as a borylene–borane adduct. However, it is notable that the B–B distance (1.789(4) Å) and the B–P distances (B2–P1 = 1.986(4), B1–P2 = 1.938(3), B1–P3 = 1.935(4) Å) are statistically indistinguishable from those in its constitutional isomer **6**, indicating that the electronic situation at the B_2 units may not be as different as these formalisms suggest.

To gain mechanistic insight into how different hydrophosphination outcomes were obtained using the diboron compounds **1–4**, DFT computations at the ωB97XD/6-31++g(d,p)/SMD//ωB97XD/6-31g(d,p) level of theory were performed. For computations, truncated models of diborenes, **A1–D1**, in which the cyclohexyl substituents of the chelating phosphines were replaced with methyl groups, were examined. The 1,1- and 1,2-hydrophosphination reactions observed are significantly exergonic, with ΔG values ranging from −23.9 to −38.4 kcal mol^{-1} (Fig. 2 and 3). For the 1,2-hydrophosphination of diborene **1**, yielding product **5**, the likely mechanism is shown in Fig. 2a. Initially, coordination of $HPPh_2$ to one of the boron atoms affords adduct **A2**. This is followed by a 1,3-H shift from the coordinated $HPPh_2$ to the distal boron atom, leading to the formation of a 1,2-hydrophosphinated intermediate **A3**, with the PPh_2 and H units located *syn* to one another. This intermediate subsequently rearranges *via* phosphine dissociation/association to form the product **A6**. For this reaction, the 1,3-H shift step was found to be rate limiting and has a barrier of 33.7 kcal mol^{-1} (**TSA(2–3)**). The calculated barrier for this pathway is seemingly high for a room-temperature reaction, and we attribute this to the use of methyl groups rather than cyclohexyl groups in the calculations. The energy reduction due to the London dispersion effect[45] from the bulky cyclohexyl groups is lost, which affects the crowded transition state more than the starting diborene. Two other reasonable mechanistic possibilities for this reaction were also explored, both of which gave higher barriers (see ESI†).

For the conversion of diborene **2** into **6**, the proposed mechanism (Fig. 2b) involves (i) an initial coordination of $HPPh_2$ to the boron centre that bears the electronegative bromide substituent and the chelating phosphine ligand, (ii) stepwise transfer (dissociation and association) of the bromide to the adjacent boron atom and (iii) 1,2-H shift from the coordinated $HPPh_2$ to the proximal boron atom, leading to the formation of 1,1-hydrophosphinated product **B5**. Here, the rate limiting step is the 1,2-H shift, which has a barrier of 31.9 kcal mol^{-1}. Our efforts to locate a transition state for a direct bromide shift from **B2** to **B4**, or to find the minimum energy structure of a bromide-bridged intermediate, were unsuccessful. All transition state optimization efforts led to dissociation of either bromide or $HPPh_2$. Minimization attempts to find the bromide-bridged intermediate led to convergence to one of the non-bridging intermediates **B2** and **B4**. Use of a highly truncated model with hydrogen substituents at all phosphorus atoms produced a single transition state for a direct bromide shift, but the free energy barrier of 66.8 kcal mol^{-1} is too high to represent a feasible mechanism (see ESI†). Thus, a dissociative pathway was proposed. Other additional mechanistic pathways were examined, but were

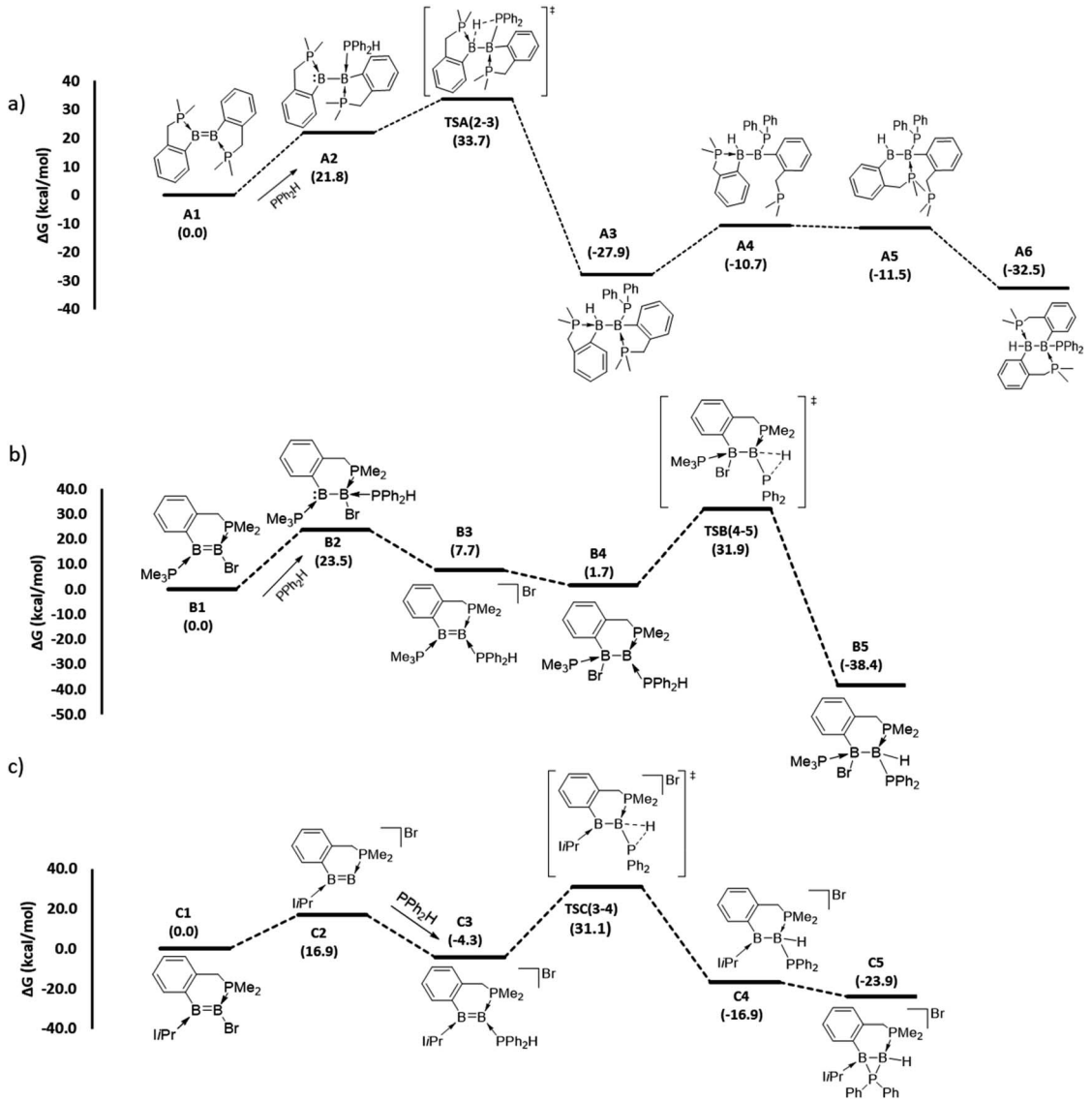

Fig. 2 DFT-computed mechanistic pathways for (a) 1,2-hydrophosphination of diborene **A1** (model of **1**), (b) 1,1-hydrophosphination of diborene **B1** (model of **2**) and (c) 1,1-hydrophosphination of diborene **C1** (model of **3**). Note: only the transition states for the rate limiting P–H bond activation steps are shown; selected representative transition states for phosphine association/dissociation steps were calculated and found to have energies marginally higher than the higher energy intermediate (see ESI†).

found to have higher barriers than that described above. We also investigated the corresponding 1,2-hydrophosphination of **B1**, which was confirmed to have a slightly higher overall barrier than the 1,1-addition.

For the cyclic product **7**, obtained from the reaction between $HPPh_2$ and the unsymmetrical, NHC-substituted diborene **3**, a similar mechanistic pathway to that of **B1** was investigated (Fig. 2c). In contrast to the **B1** case, complexation of $HPPh_2$ to diborene **C1** only occurs after initial dissociation of the bromide ion. This difference can be primarily attributed to the large steric hindrance exerted by the two isopropyl peripheries of the NHC ligand as well as ample charge flow from the NHC to the distal boron centre. Unlike in **B1**, the dissociated bromide cannot feasibly bind to the adjacent boron in cationic intermediate **C3**, again due to the strong electron donation and steric hindrance of the NHC ligand. As a result, **C3** is forced to undergo a 1,2-proton shift from the coordinated $HPPh_2$, leading to the formation of 1,1-hydrophosphinated cationic intermediate **C4**, with the positive charge predominantly localised at the NHC-coordinated boron centre. As a means to alleviate the electron deficiency at this boron centre, in the subsequent step the phosphinyl substituent establishes a dative interaction, leading to the observed product **C5**. For this reaction, an overall barrier of 31.1 kcal mol^{-1} was found for the 1,2-H shift step.

The mechanistic pathway for the 1,2-hydrophosphination of borylborylene **4** to form **8** can be described straightforwardly (Fig. 3). Given that the boron atom of the boryl unit holds a partial positive charge (*vide infra*), it can easily bind the incoming phosphine. The resulting loss of π-delocalisation of the borylene lone pair leaves it strongly localised, and in the

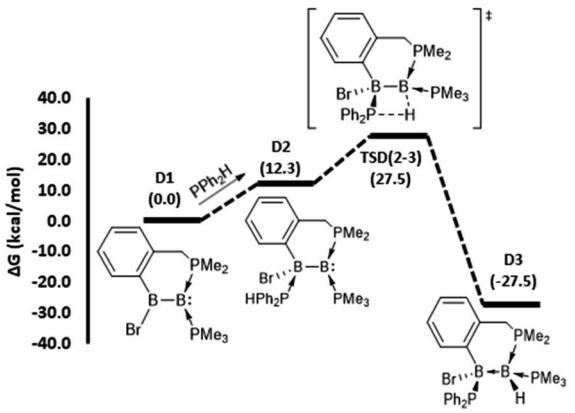

Fig. 3 DFT-computed mechanistic pathways for 1,2-hydrophosphination of borylborylene **D1** (model of **4**). Note: the transition state between **D1** and **D2** was found to have a very low barrier (14.3 kcal mol^{-1}) and is not shown.

ensuing step a protic 1,3-H shift from the $HPPh_2$ unit to the borylene boron atom occurs, affording the product **D3**. This rate limiting step has a barrier of only 27.5 kcal mol^{-1}, which is the lowest among the reactions investigated. Notably, the inverse addition of the P–H bond across the diborene is strongly disfavoured (see ESI†), supporting the selectivity to the observed product.

To understand why diborene **1** and borylborylene **4** prefer 1,2-hydrophosphination, while diborenes **2** and **3** undergo 1,1-hydrophosphination, a selection of NPA partial charges were analysed (Table 1). The symmetrical diborene **A1** displays partial negative charge on both boron atoms (entry 2, parentheses), as expected for diborenes.[46] In line with our previous analysis of the Hirshfeld charges of the unsymmetrical species **2–4**,[37] the NPA partial charges of the model diborenes **B1** and **C1** and borylborylene **D1** (parentheses of entries 3–5) displayed a very similar trend for the charge accumulation and the course of charge flow on the boron atoms. Upon coordination of $HPPh_2$ to the electron-rich diborene **C1**, the negative charges on both boron atoms increase further, with a relatively high negative charge localised on B_{DIST} (the boron atoms are denoted as B_{PROX} and B_{DIST}, respectively, for those proximal and distal to the incoming $HPPh_2$). Simultaneously, the partial positive charge at the $HPPh_2$ phosphorus atom increases, confirming the charge donation from the incoming phosphine. Another intriguing fact about the coordinated $HPPh_2$ is that its hydrogen substituent obtains a partial positive charge in contrast to its free form, which is marginally negative at hydrogen (entry 1). Thus, it is apparent that the hydrogen transfer from phosphorus to boron during hydrophosphination is a proton transfer, not a hydride transfer. As anticipated, the $HPPh_2$ coordination **A1–D1** is endergonic due to addition of a weak phosphine nucleophile to an electron-rich diborene. As the initially formed phosphine adducts of diborene **A1** and borylborylene **D1** are the immediate precursors to the transition states that involve a proton shift step, the partial charges at both boron atoms of these intermediates (**A2** and **D2**) were analyzed. The adduct **A2** shows a high negative charge build-up on the boron atom distal to the coordinated $HPPh_2$ (entry 2). As a result, B_{DIST} abstracts the proton from the coordinated $HPPh_2$. Likewise, the localized high negative charge on B_{DIST} in intermediate **D2** (entry 5) drives the proton shift to this distal boron. For the reaction coordinates of diborenes **B1** and **C1**, the immediate precursors to the proton transfer transition state are **B4** and **C3**, respectively. In these two intermediates (entries 3 and 4), a high negative charge build-up was found on B_{PROX} (bound to $HPPh_2$), leading in both cases to 1,1-hydrophosphination.

Table 1 Computed NPA partial charges (q) on selected atoms of diborenes and intermediates immediately prior to the transition states that involve a proton shift[a]

Entry	Species	q (H)	q ($P_{(PPh_2H)}$)	q (B_{PROX})	q (B_{DIST})
1	PPh_2H	−0.02	0.613	—	—
2	**A2**	0.041	1.138	−0.468 (−0.324)	−0.611 (−0.324)
3	**B4**	0.044	1.155	−1.230 (−0.451)	−0.113 (−0.453)
4	**C3**	0.017	1.197	−1.061 (−0.546)	0.222 (−0.102)
5	**D2**	0.005	1.117	−0.055 (0.298)	−1.238 (−1.205)

[a] B_{PROX} refers to the PPh_2H-coordinated boron atom, whereas B_{DIST} refers to the other boron atom. The charges in parentheses are of the boron atoms of starting diborenes.

Overall, these computations show that the hydrophosphination of diborenes begins with an initial coordination of the substrate $HPPh_2$ to the boron atoms of electron-rich diborenes, followed by a proton shift from the coordinated $HPPh_2$ to the proximal or distal boron, depending on which has a higher localised negative partial charge, dictating whether the 1,1- or 1,2-hydrophosphinated product is obtained.

Recent success in adding B–B and B–H bonds across boron–boron triple bonds[32,34] led us to consider the hydrophosphination of diborynes. We chose the least sterically encumbered diboryne currently available, $B_2(SI^{Dep})_2$ (**9**, SI^{Dep} = 1,3-bis(2,6-diethylphenyl)imidazolin-2-ylidene),[28] in the hope that this would allow the approach of the relatively bulky substrate. Treatment of **9** with excess $HPPh_2$ at −78 °C in toluene (Scheme 3) resulted in an immediate colour change from red to purple. After warming to room temperature, analysis by NMR spectroscopy revealed clean conversion to a new species with a doublet signal at −25.9 ppm (J = 46 Hz) in the ^{31}P NMR spectrum. Two broad resonances were observed at 38.3 and 18.0 ppm in the ^{11}B NMR spectrum, shifted significantly from that of **9** (δ = 55.9 ppm) and in the expected region for diborenes. The $^{1}H\{^{11}B\}$ NMR spectrum exhibited a conspicuous

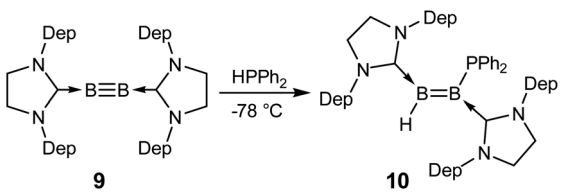

Scheme 3 Hydrophosphination of the boron–boron triple bond in a diboryne. Dep = 2,6-diethylphenyl.

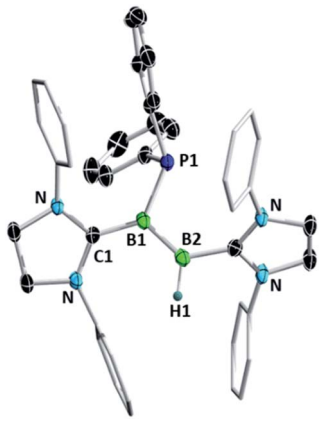

Fig. 4 Molecular structure of compound **10** with selected atomic displacement ellipsoids at the 50% probability level. Hydrogen atoms except for H1, ethyl groups and a co-crystallised hexane molecule are omitted for clarity. Selected bond lengths (Å) and torsions (°): B1–B2 1.567(3), B1–P1 1.945(2), B1–C1 1.553(3), B2–C2 1.583(3), C1–B1–B2–B1 177.1(2).

broadened doublet at 4.19 ppm, indicating a boron-bound proton coupled to the phosphorus nucleus ($^3J_{PH}$ = 46 Hz). Crystals obtained from a pentane solution allowed determination of the structure of the compound (Fig. 4). The product, diborene **10**, is the result of a 1,2-hydrophosphination across the boron–boron triple bond. Compound **10** is the first example of a phosphinodiborane. The B–B bond distance of 1.567(3) Å is somewhat shorter than in the related hydro(boryl)diborene $SI^{DipMes}(H)B{=}B(Bcat)SI^{DipMes}$ (SI^{DipMes} = 1-(2,4,6-trimethylphenyl)-3-(2,6-diisopropylphenyl)-imidazolin-2-ylidene, B=B = 1.609(2) Å),[32] while the B1–P1 distance is shorter than that in phosphinodiboranes **5–8**, at 1.945(2) Å, on account of the sp^2 hybridisation at boron.

No further reaction of **10** with $HPPh_2$ could be observed, even after heating the sample to 100 °C in toluene solution, in stark contrast to the behaviour of compounds **1–4**. We ascribe this lack of reactivity to the large steric bulk of the flanking NHC ligands when compared to the accessible boron–boron bonds of the benzylphosphine-supported species.

Conclusion

In summary, we have demonstrated that diborenes undergo catalyst-free hydrophosphination reactions with diphenylphosphine under mild conditions. The substituents at the diborene dictate whether the reaction proceeds as a 1,1- or 1,2-addition. The major influencing factor for the regiochemistry appears to be the relative partial charges at the boron atoms in the initial adduct. We have also reported 1,2-hydrophosphination of a diboryne, yielding an unsymmetrical hydro(phosphino)diborene. Our current efforts are focussed on exploring more challenging σ-bond activations at these highly reactive boron–boron multiple bonds.

Conflicts of interest

There are no conflicts to declare.

Acknowledgements

We gratefully acknowledge the European Research Council for funding under the European Union Horizon 2020 Research and Innovation Program (grant agreement no. 669054). A. J. thanks the government of Canada for an NSERC postdoctoral fellowship.

Notes and references

1 J. A. Bailey and P. G. Pringle, *Coord. Chem. Rev.*, 2015, **297**, 77–90.
2 D. C. Pestana and P. P. Power, *J. Am. Chem. Soc.*, 1991, **113**, 8426–8437.
3 R. T. Paine and H. Nöth, *Chem. Rev.*, 1995, **95**, 343–379.
4 X. D. Feng, M. M. Olmstead and P. P. Power, *Inorg. Chem.*, 1986, **25**, 4615–4616.
5 For the sake of consistency, we have used the definitions of Bailey and Pringle (ref. 1) to make the distinction between the two structural extremes of monomeric P–B compounds.
6 J. M. Breunig, A. Hubner, M. Bolte, M. Wagner and H. W. Lerner, *Organometallics*, 2013, **32**, 6792–6799.
7 S. J. Geier, T. M. Gilbert and D. W. Stephan, *J. Am. Chem. Soc.*, 2008, **130**, 12632–12633.
8 A. Amgoune, S. Ladeira, K. Miqueu and D. Bourissou, *J. Am. Chem. Soc.*, 2012, **134**, 6560–6563.
9 A. M. Spokoyny, C. D. Lewis, G. Teverovskiy and S. L. Buchwald, *Organometallics*, 2012, **31**, 8478–8481.
10 J. A. Bailey, M. F. Haddow and P. G. Pringle, *Chem. Commun.*, 2014, **50**, 1432–1434.
11 J. A. Bailey, M. Ploeger and P. G. Pringle, *Inorg. Chem.*, 2014, **53**, 7763–7769.
12 D. Dou, G. W. Linti, T. Q. Chen, E. N. Duesler, R. T. Paine and H. Nöth, *Inorg. Chem.*, 1996, **35**, 3626–3634.
13 T. Q. Chen, E. N. Duesler, R. T. Paine and H. Nöth, *Inorg. Chem.*, 1999, **38**, 4993–4999.
14 T. Q. Chen, E. N. Duesler, H. Nöth and R. T. Paine, *J. Organomet. Chem.*, 2000, **614**, 99–106.
15 S. J. Geier, T. M. Gilbert and D. W. Stephan, *Inorg. Chem.*, 2011, **50**, 336–344.
16 A. Lik, D. Kargin, S. Isenberg, Z. Kelemen, R. Pietschnig and H. Helten, *Chem. Commun.*, 2018, **54**, 2471–2474.
17 M. Kaaz, C. Baucker, M. Deimling, S. König, S. H. Schlindwein, J. Bender, M. Nieger and D. Gudat, *Eur. J. Inorg. Chem.*, 2017, **2017**, 4525–4532.
18 A. Ordyszewska, N. Szynkiewicz, E. Perzanowski, J. Chojnacki, A. Wiśniewska and R. Grubba, *Dalton Trans.*, 2019, **48**, 12482–12495.
19 G. E. Coates and J. G. Livingstone, *J. Chem. Soc.*, 1961, 1000–1008.
20 M. Kaaz, J. Bender, D. Forster, W. Frey, M. Nieger and D. Gudat, *Dalton Trans.*, 2014, **43**, 680–689.
21 A. D. Gorman, J. A. Bailey, N. Fey, T. A. Young, H. A. Sparkes and P. G. Pringle, *Angew. Chem., Int. Ed.*, 2018, **57**, 15802–15806.
22 O. Delacroix and A. C. Gaumont, *Curr. Org. Chem.*, 2005, **9**, 1851–1882.

23 D. S. Glueck, *Top. Organomet. Chem.*, 2010, **31**, 65–100.
24 I. Wauters, W. Debrouwer and C. V. Stevens, *Beilstein J. Org. Chem.*, 2014, **10**, 1064–1096.
25 S. Greenberg and D. W. Stephan, *Chem. Soc. Rev.*, 2008, **37**, 1482–1489.
26 S. Harder, *Chem. Rev.*, 2010, **110**, 3852–3876.
27 G. Hong, X. Y. Zhu, C. Hu, A. N. Arum, S. Y. Wu and L. M. Wang, *J. Org. Chem.*, 2016, **81**, 6867–6874.
28 M. Arrowsmith, J. Böhnke, H. Braunschweig, M. A. Celik, T. Dellermann and K. Hammond, *Chem.–Eur. J.*, 2016, **22**, 17169–17172.
29 J. H. Muessig, M. Thaler, R. D. Dewhurst, V. Paprocki, J. Seufert, J. D. Mattock, A. Vargas and H. Braunschweig, *Angew. Chem., Int. Ed.*, 2019, **58**, 4405–4409.
30 H. Braunschweig, R. D. Dewhurst, C. Hörl, A. K. Phukan, F. Pinzner and S. Ullrich, *Angew. Chem., Int. Ed.*, 2014, **53**, 3241–3244.
31 H. Braunschweig and C. Hörl, *Chem. Commun.*, 2014, **50**, 10983–10985.
32 T. Brückner, T. E. Stennett, M. Heß and H. Braunschweig, *J. Am. Chem. Soc.*, 2019, **141**, 14898–14903.
33 T. E. Stennett, R. Bertermann and H. Braunschweig, *Angew. Chem., Int. Ed.*, 2018, **57**, 15896–15901.
34 T. Brückner, R. D. Dewhurst, T. Dellermann, M. Müller and H. Braunschweig, *Chem. Sci.*, 2019, **10**, 7375–7378.
35 H. Braunschweig, P. Constantinidis, T. Dellermann, W. C. Ewing, I. Fischer, M. Hess, F. R. Knight, A. Rempel, C. Schneider, S. Ullrich, A. Vargas and J. D. Woollins, *Angew. Chem., Int. Ed.*, 2016, **55**, 5606–5609.
36 J. Böhnke, T. Dellermann, M. A. Celik, I. Krummenacher, R. D. Dewhurst, S. Demeshko, W. C. Ewing, K. Hammond, M. Heß, E. Bill, E. Welz, M. I. Rohr, R. Mitric, B. Engels, F. Meyer and H. Braunschweig, *Nat. Commun.*, 2018, **9**, 1197.
37 T. E. Stennett, J. D. Mattock, I. Vollert, A. Vargas and H. Braunschweig, *Angew. Chem., Int. Ed.*, 2018, **57**, 4098–4102.
38 T. E. Stennett, J. D. Mattock, L. Pentecost, A. Vargas and H. Braunschweig, *Angew. Chem., Int. Ed.*, 2018, **57**, 15276–15281.
39 R. D. Dewhurst, E. C. Neeve, H. Braunschweig and T. B. Marder, *Chem. Commun.*, 2015, **51**, 9594–9607.
40 J. Böhnke, M. Arrowsmith and H. Braunschweig, *J. Am. Chem. Soc.*, 2018, **140**, 10368–10373.
41 J. B. Bourg, A. Rodriguez, D. Scheschkewitz, H. Gornitzka, D. Bourissou and G. Bertrand, *Angew. Chem., Int. Ed.*, 2007, **46**, 5741–5745.
42 A. Rodriguez, F. S. Tham, W. W. Schoeller and G. Bertrand, *Angew. Chem., Int. Ed.*, 2004, **43**, 4876–4880.
43 A. Rodriguez, G. Fuks, J. B. Bourg, D. Bourissou, F. S. Tham and G. Bertrand, *Dalton Trans.*, 2008, 4482–4487, DOI: 10.1039/b718631b.
44 W. Lu, K. Xu, Y. X. Li, H. Hirao and R. Kinjo, *Angew. Chem., Int. Ed.*, 2018, **57**, 15691–15695.
45 J. P. Wagner and P. R. Schreiner, *Angew. Chem., Int. Ed.*, 2015, **54**, 12274–12296.
46 M. Arrowsmith, H. Braunschweig and T. E. Stennett, *Angew. Chem., Int. Ed.*, 2017, **56**, 96–115.